Polarization of amplified spontaneous emission in a plasma active medium

C. M. Kim,[1,2] H. Stiel,[3] B. Matouš,[4] M. Nishikino,[5] N. Hasegawa,[5] T. Kawachi,[5] K. A. Tran,[6] and K. A. Janulewicz[6,1,*]

[1]*Center for Relativistic Laser Science, Institute for Basic Science (IBS), Gwangju 500-712, Republic of Korea*

[2]*Advanced Photonics Research Institute, Gwangju Institute of Science and Technology (GIST), Gwangju 500-712, Republic of Korea*

[3]*Max-Born Institute (MBI), D-12489 Berlin, Germany*

[4]*Czech Technical University, Prague 6, Czech Republic*

[5]*Advanced Photonics Research Center, Japan Atomic Energy Agency (JAEA), Kyoto 619-0215, Japan*

[6]*Department of Physics and Photon Science, Gwangju Institute of Science and Technology (GIST), Gwangju 500-712, Republic of Korea*

(Received 8 April 2015; published 6 October 2015)

We present polarization measurement of a Ni-like Ag x-ray laser working in the transient collisional excitation scheme. A calibrated membrane multilayer beam splitter was used to determine the energies of two mutually perpendicular polarization components (s and p components). As a result, we observed a high degree of polarization that fluctuated from shot to shot. The dominant polarization component switched from s to p when pumping was made stronger. The measurement results are discussed from the point of view of the general polarization theory and supported by a numerical simulation based on Maxwell-Bloch equations. The physical processes causing the dominance of one polarization component are discussed in terms of pumping strength. These results should extend the wave physics perspective on the amplification process, transforming a weak random noise into a strong coherent radiation.

DOI: 10.1103/PhysRevA.92.043807 PACS number(s): 42.55.Vc, 42.25.Ja, 42.25.Bs

I. INTRODUCTION

During the last few decades, x-ray lasers (XRLs) based on laser-produced plasmas have been widely studied due to their unique features in extreme ultraviolet (EUV) and soft x-ray spectral regions [1–3]. The specific radiation parameters of XRLs such as short wavelength, high temporal coherence, high photon flux, and short pulse duration are extremely valuable to many applications on fine spatiotemporal scales [4–9]. In parallel with the practical aspects, the fundamental aspects of XRL physics have been studied extensively. Now, the basic physical processes underlying XRLs, e.g., laser-plasma interaction, gain dynamics of plasma active mediums, and propagation of amplified spontaneous emission (ASE), are understood reasonably well [2,10,11].

Knowledge of XRL polarization, being one of the fundamental characteristics of any radiation source, lags behind that related to other main source parameters like pulse energy, coherence, and pulse duration. This deficit appeared mainly due to the lack of commercial efficient polarizers and compensators in the considered spectral region. In addition, since ASE originates from random noise, and the electron collision frequency is high in the plasma medium, XRLs have been presumed to have undefined polarization.

Up to now, only two groups have reported on the measurements of XRL polarization, albeit their results were contradictory. Kawachi *et al.* reported a high degree of polarization (DOP) and dominance of s component when two laser pulses pumped the medium in the quasi-steady-state (QSS) regime [12]. On the contrary, Rus *et al.* claimed unpolarized output from a QSS XRL pumped by a single, long laser pulse [13]. In the explanation delivered in Ref. [12], the anisotropic radiation trapping of the nonlasing resonance transition involving the lower lasing level and consequent population imbalance accounted for the production of a higher gain for the s component. In Ref. [13], the population equilibration among the states of the lower level, caused by strong electron collisions, was considered to quench any polarization effect [14]. However, the assumed collision frequency was higher by several orders of magnitude than that typically estimated from linewidth broadening. As for the XRLs based on transient collisional excitation (TCE) scheme, which greatly reduced the pumping energy threshold (compared to QSS XRLs) and thus has become the most commonly used scheme, no results have been reported.

All the previously reported results were formulated and processed by applying the conventional expression of DOP based on the energies contained in s and p perpendicular components. In principle, the phase correlation between the two components was neglected. In such a case, the DOP is given by the formula $\mathcal{P}_u = |1 - r|/(1 + r)$ where r refers to the ratio of the energy contained in one component to that in the other component. However, according to a recent theoretical study using Maxwell-Bloch equations [15], the phase correlation can be substantial even when no significant coupling occurs between the lasing transitions producing the polarization components. Hence, a proper analysis of XRL polarization should take the phase correlation into account as in the rigorous theory of polarization [16]. The inappropriateness of the formula in general cases is obvious when it is applied to a circularly polarized radiation.

In the present paper, we report on the polarization measurement in the output beam of a Ni-like Ag XRL based on the TCE scheme. The measured DOP ($\mathcal{P}_u$) was high and fluctuating from shot to shot. The dominant polarization component switched from s to p when pumping was made stronger. The physical processes underlying the observations are discussed in detail, and the relation between measured DOP ($\mathcal{P}_u$) and the generalized DOP incorporating phase correlation is analyzed by using a simulation based on Maxwell-Bloch equations.

*kaj@gist.ac.kr

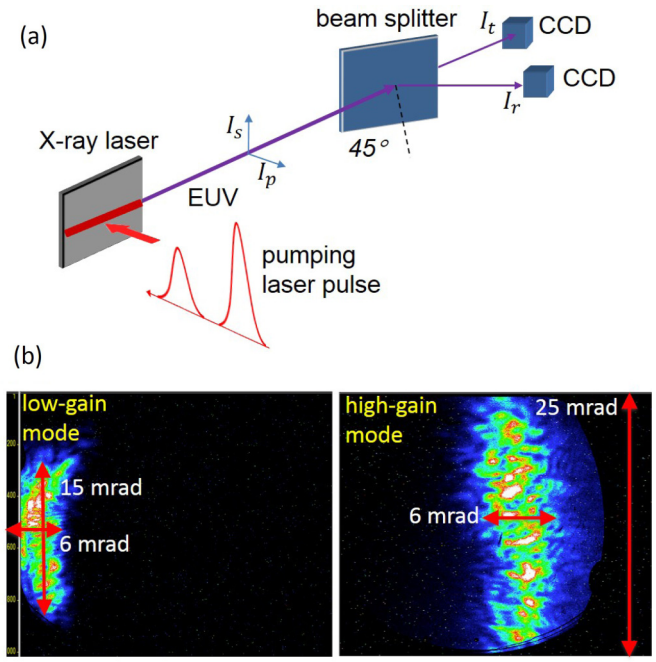

FIG. 1. (Color online) (a) Experimental setup for measuring XRL polarization. I_s and I_p refer to the energies in the s and p polarization components of the XRL radiation incident, respectively, at 45° into the beam splitter. I_r and I_t refer to the measured energy of the reflected and transmitted beams, respectively, measured by the two CCDs. (b) The beam patterns of the low-gain mode and the high-gain mode, measured about 1 m away from the targets. The red arrows show the lengths corresponding to the marked divergence values.

II. METHODS

Polarization experiments were carried out using a Ni-like Ag XRL operating in a classical double-pulse arrangement of the TCE scheme [17,18]. A membrane soft x-ray beam splitter (BS) [19] was used to determine the mutually perpendicular polarization components. The strong dependence of reflection characteristics of BS on the polarization state of radiation was exploited in the measurement. The experimental setup is described in more detail in Refs. [17,18].

Two IR laser pulses (prepulse and main pulse) of a duration of 4 ps, separated by 2.4 ns, irradiated normally an Ag slab target to create a line focus, as shown in Fig. 1(a). An XRL pulse of a central wavelength equal to 13.9 nm was developed along the created plasma column. The XRL was operated at two different conditions: low-gain mode and high-gain mode. The low-gain mode was obtained with a total pumping energy of 3.4 J (0.4-J variation), a contrast (ratio of the prepulse energy to that of the main pulse) of 0.2, and a focusing area of 8.8 mm $\times 10$ μm (measured in air with 1-mJ laser energy without a target). The peak intensities of the prepulse and the main pulse were estimated to be 9.5×10^{13} and 3.8×10^{14} W/cm^2, respectively. The target width limited the gain medium length to 7 mm. The small-signal gain coefficient (g_0) was measured to be 20 cm^{-1}, resulting in a gain-length product ($g_0 l$) of 14. The total radiation energy was about 1 μJ. The vertical and horizontal beam divergences were 15 and 6 mrad, respectively, as shown in Fig. 1(b). In contrast, the high-gain mode was obtained with a higher total pumping energy of 4.5 J (0.4-J variation), a contrast of 0.1, and a focusing area of 8.3 mm $\times$ 25 μm. The peak intensities of the prepulse and the main pulse were estimated to be 2.7×10^{13} and 2.4×10^{14} W/cm^2, respectively. The medium length was the same. The small-signal gain coefficient was not directly measured but estimated from our previous detailed measurements in the same setup: $g_0 = 42\,\text{cm}^{-1}$ and $g_0 l = 29$ [20,21]. The total radiation energy was about 1 μJ. The vertical and horizontal beam divergences were 25 and 6 mrad, respectively, as shown in Fig. 1(b). According to our previous measurements in the same setup [17,20] and the typical saturation criterion for this type of XRLs $g_0 l = 15$ [10], the low-gain mode can be considered as unsaturated or weakly saturated and the high-gain mode fully saturated. The results of our simulation also support this consideration, as it can be seen in Fig. 4.

The difference between the two regimes appeared mainly due to the difference in the prepulse level. When a prepulse impinges on a target surface, it generates a plasma that expands until the main pulse arrives (for 2.4 ns in our case). If the prepulse is strong (e.g., 9.5×10^{13} W/cm^2 for the low-gain mode), the plasma is hot and expands rapidly, giving in the final effect a long density scale length. Consequently, the main pulse heats a large volume of a low-density plasma, resulting in a low-gain regime with a large cross section. On the other hand, if the prepulse is weaker (e.g., 2.7×10^{13} W/cm^2 for the high-gain mode), the plasma is relatively cold and expands less. Consequently, a small volume of a high density is heated by the main pulse, resulting in a high-gain mode with a small cross section. In our arrangement, the change in the prepulse level was implemented by varying the focal width. It is a simple way to adjust the density and size of the preplasma without significant changes in the laser parameters.

It is worth noting that the total radiation energy from the low-gain mode can be comparable to that from the high-gain mode because it has a larger cross section, as in our case. The difference in cross section between the two modes results in the difference in beam divergence, as illustrated in Fig. 1(b): the low-gain mode produces a smaller beam divergence due to its larger cross section.

After propagating over a distance over 4 m, the XRL pulse was split by the BS into reflected and transmitted pulses with energies I_r and I_t measured by two soft x-ray–sensitive CCDs (Princeton Instruments, back-illumination type, 13.5 μm/pixel). Since the active area of the BS with a dimension of 6 $\times$ 6 mm was much smaller than the beam diameter at this position (20–32 mm estimated by assuming a divergence of 5–8 mrad typical for this type of XRL), a sort of mode selection was introduced in the experimental setup. Due to selecting a small beam area for data acquisition, the recorded x-ray flux passing through the window of the BS can be smaller for a beam with larger divergence, as can be seen in Figs. 2 and 3. Additionally, a mode-selection-like procedure was imposed by using in the data processing an area of only 40 $\times$ 40 pixels (corresponding to 540 $\times$ 540 μm) around the signal peak on the CCD sensor.

Since accurate knowledge of the BS characteristics is crucial, the BS was carefully calibrated. The reflectance and

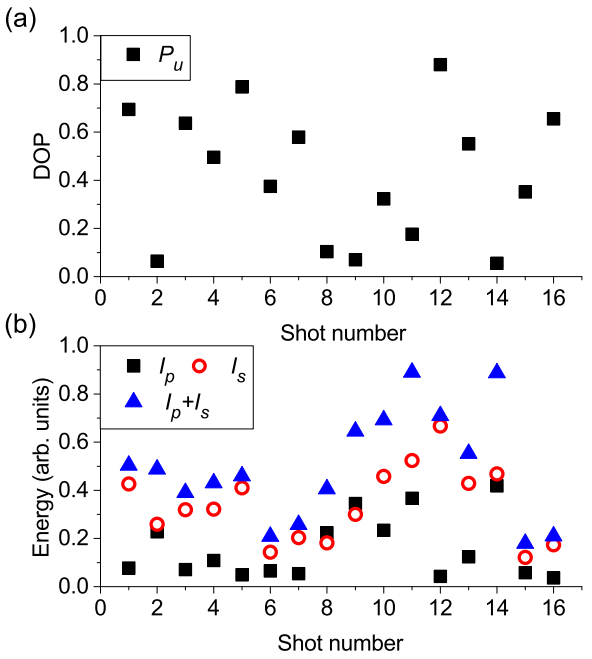

FIG. 2. (Color online) Measurement of polarization at the low-gain regime: (a) DOP and (b) the energy in each polarization component and the total energy. The descriptive statistics of the data are as follows: $\langle \mathcal{P}_u \rangle = 0.42$, $\delta \mathcal{P}_u = 0.27$, $\langle I_p \rangle = 0.16$, $\delta I_p = 0.13$, $\langle I_s \rangle = 0.34$, $\delta I_s = 0.15$, $\langle I_p + I_s \rangle = 0.49$, and $\delta(I_p + I_s) = 0.23$.

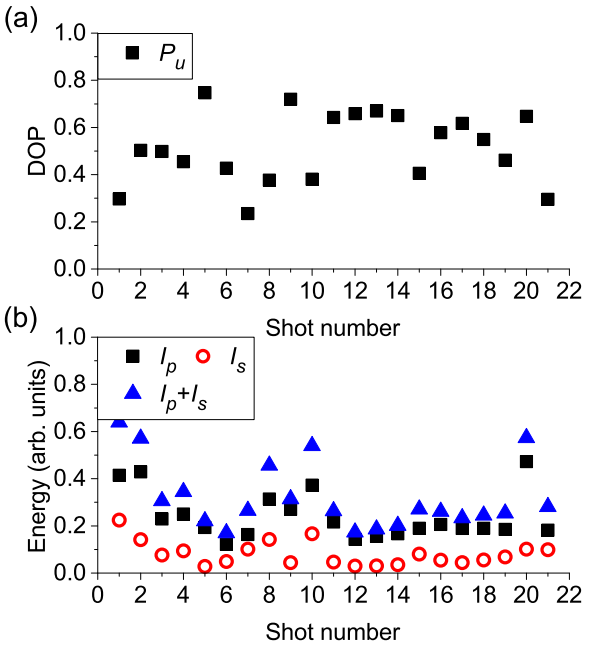

FIG. 3. (Color online) Measurement of polarization at the high-gain regime: (a) DOP and (b) the energy in each polarization component and the total energy. The descriptive statistics of the data are as follows: $\langle \mathcal{P}_u \rangle = 0.52$, $\delta \mathcal{P}_u = 0.15$, $\langle I_p \rangle = 0.24$, $\delta I_p = 0.10$, $\langle I_s \rangle = 0.08$, $\delta I_s = 0.05$, $\langle I_p + I_s \rangle = 0.32$, and $\delta(I_p + I_s) = 0.14$. The energy scale in this figure is the same as that in Fig. 2.

transmittance for s polarization, designated by R_s and T_s, respectively, were measured at a synchrotron beamline of PTB Berlin [22]. The BS consisted of a protective layer on the top, a Mo-Si multilayer in the middle, and a Si_3N_4 substrate at the bottom. The coating has negligible absorption, and the substrate has negligible reflection and does not affect polarization [19]. The transmission value T_0 of the Si_3N_4 substrate was calculated to be 0.2 [23]. Then R_p and T_p were calculated from R_s, T_s, T_0, and the tabulated scattering factors [23]. As a result, the values of the complete BS parameters were $R_s = 0.20$, $T_s = 0.16$, $R_p = 0.002$, and $T_p = 0.2$. Using these, the values of I_s and I_p were obtained from the recorded values of I_r and I_t: $I_s = (R_p I_t - T_p I_r)/(T_s R_p - T_p R_s)$ and $I_p = (T_s I_r - R_s I_t)/(T_s R_p - T_p R_s)$. It is worth noting that these characteristics were also verified with an incoherent soft x-ray source.

III. RESULTS AND DISCUSSION

A. Polarization measurements

The polarization measurements performed at the aforementioned two different regimes gave clearly different XRL output characteristics. The high-gain regime produced a strong but divergent output signal and the other generated a weaker but more directional signal, as shown in Fig. 1(b). The two regimes resulted in quite different polarization states of the output radiation, suggesting a significant dependence of polarization on the pumping condition.

For the low-gain regime, we observed a significant but fluctuating DOP and dominance of s polarization, as shown in Fig. 2: $\langle \mathcal{P}_u \rangle = 0.42$, $\delta \mathcal{P}_u = 0.27$, and $\langle I_s \rangle / \langle I_p \rangle = 2.1$, where $\langle A \rangle$ and δA refer to the mean and the standard deviation of a random variable A, respectively. Except when the DOP is small ($\leqslant 0.1$, two shots out of 16 shots), the s polarization component is stronger than the p polarization component: the energy ratio $r = I_s/I_p$ varies between 0.8 and 16, with a median of 2.6. The variation in r causes the corresponding variation in DOP $\delta \mathcal{P}_u$, as it can be inferred from the formula $\mathcal{P}_u = |1 - r|/(1 + r)$. It should be noted that a given value of r and its reciprocal give the same value of $\mathcal{P}_u$. The total energy shows a substantial level (0.47) of relative fluctuation (ratio of the standard deviation to the mean), consistent with the fact that we consider this regime unsaturated or weakly saturated.

The dominance of s polarization, $\langle I_s \rangle / \langle I_p \rangle = 2.1$ for the data shown in Fig. 2(b), is reasonably consistent with the result reported by Kawachi *et al.* [12], where $I_s/I_p = 3.3$ measured with a pump laser energy of 170 J and $I_s/I_p = 1.5$ with an energy of 190 J. But the width of the line focus was 100 μm, about 4 times broader than that in the present experiments. Such a directional effect was ascribed to the anisotropy in atomic kinetics and plasma dynamics. The steep ion velocity gradient induced by the plasma stream normal to the target was proposed in Ref. [12], based on a hydrodynamics simulation as the reason for such a behavior. In this case, the spatial variation in the Doppler shift causes a population imbalance among the states of the lower lasing level. This imbalance is a result of a differential radiation trapping of the nonlasing transition involving the lower lasing level. Since the TCE scheme used in our experiments produced a plasma medium with a higher gain and steeper density gradients compared

to the QSS scheme used in Refs. [12,13], the hydrodynamic origin proposed in Ref. [12] could be even more effective in this case.

Another argument for the dominance of s polarization was given by Dubau *et al.* [24], who considered a beam of hot ($E \sim$ keV) electrons generated normally to the target during plasma heating. If such an electron beam is sufficiently dense (5%–10% of bulk), it can cause a population imbalance among the states of the lower lasing level for the experimental condition reported in Ref. [12]. Their radiation transfer simulation incorporating a collisional-radiative model clearly showed such a possibility. This argument was based on prominent research on the electron distribution in a laser-produced plasma [25,26], which demonstrated and elucidated how spatially anisotropic electron distribution makes the radiation from laser-produced plasmas polarized; the effect has been known in discharge plasmas for 90 years [27,28]. Generation of such a hot anisotropic electron distribution is attributed to the steep temperature gradient in the conduction zone [25,26], which is, however, denser by at least 1 order of magnitude than the region where x-ray lasing occurs. Furthermore, since XRL media are heated dominantly by inverse bremsstrahlung, they have little chance of developing such a hot region in the vicinity of the conduction zone. In addition, the use of a monoenergetic electron beam in the model seems to be far from realistic conditions. In these regards, we consider the argument in Ref. [24] as inappropriate for explaining the dominance of s polarization.

In contrast, we observed for the high-gain regime a higher DOP with reduced fluctuation and dominance of p polarization, as shown in Fig. 3: $\langle \mathcal{P}_u \rangle = 0.52$, $\delta \mathcal{P}_u = 0.15$, and $\langle I_s \rangle / \langle I_p \rangle = 0.33$. All shots showed dominance of p polarization as r varied between 0.14 and 0.62 with a median of 0.33. The relative fluctuation of the total energy is 0.44, similar to the low-gain regime, but some consecutive shots (e.g., shots 12–19) showed higher energy stability (a relative fluctuation of 0.16). The pumping laser energy variation was 4.5% for all the shots in Fig. 3 but 2.8% for shots 12–19. This seems to be consistent with considering the high-gain regime as saturated. As mentioned in Sec. II, the absolute value of the signal level in Fig. 3(b) is lower than that in Fig. 2(b) due to the larger beam divergence of the high-gain regime and the window-limiting measurement. Unfortunately, the arguments presented above for the low-gain regime do not explain the dominance of p polarization. Compared to the low-gain regime, the high-gain regime should produce a stronger anisotropy along the target normal direction, i.e., the field direction of the p-polarized component. The question arises as to whether and how much pronounced hydrodynamics due to stronger pumping can force the dominance of a specific polarization component.

B. Degree of polarization with phase correlation

Considering that stimulated emission, the fundamental mechanism in laser amplifiers, is a coherent process by nature, a high value of DOP implies a significant level of phase correlation, the effect which is neglected in $\mathcal{P}_u$. To discuss the general case including phase correlation, one needs to use the rigorous theory of polarization formulated in Ref. [16]. According to this theory, the polarization of radiation is described in terms of the polarization matrix J:

$$J = \begin{pmatrix} \overline{E_s^*(t)E_s(t)} & \overline{E_s^*(t)E_p(t)} \\ \overline{E_p^*(t)E_s(t)} & \overline{E_p^*(t)E_p(t)} \end{pmatrix},$$

where $E_i(t)$ is the complex amplitude of the electric field polarized along the i axis, and the overbar means integration in time domain. Using the definition $J_{ij} \equiv \overline{E_i^*(t)E_j(t)}$, the energy in the polarization component along the i axis is given as $J_{ii} = I_i$ up to a common factor. We rewrite J in a more suitable form:

$$J = J_{pp} \begin{pmatrix} r & \sqrt{r\rho}e^{i\phi} \\ \sqrt{r\rho}e^{-i\phi} & 1 \end{pmatrix},$$

where $\sqrt{\rho}e^{i\phi} = J_{sp}/\sqrt{J_{pp}J_{ss}}$. In this form, r is the energy ratio I_s/I_p, and ρ ($0 \leqslant \rho \leqslant 1$) represents the degree of phase correlation. Then the generalized DOP is given as $\mathcal{P} = \sqrt{\{(1-r)^2 + 4r\rho\}}/(1+r)^2$, which always satisfies the relation $\mathcal{P} \geqslant \mathcal{P}_u$. The equality holds when the phase correlation is neglected, i.e., $\rho = 0$. Measurement of $\mathcal{P}$, i.e., determining r and ρ, requires the presence of both a polarizer and a compensator (or their equivalents) [16], of which combination is hardly available in the spectral regions of EUV and soft x rays.

We tried to compensate at least partly the lack of means to measure $\mathcal{P}$, resorting to a simulation based on the one-dimensional Maxwell-Bloch equations [15]. The equations fully take into account the wave properties of radiation and matter. The spontaneous emission was emulated as short wavelets having random phase and polarization. The simulation parameters were chosen to match the typical values of the macroscopic parameters observed in the experiments [17,29–31]: small-signal coefficients (g_0) of 20 cm^{-1} and 40 cm^{-1} for the low-gain regime and the high-gain regime, respectively. A medium length (l) of 7 mm and a gain duration of 15 ps reasonably followed the experimental values. Other parameters, mostly microscopic parameters, were identical to those used in the simulation of a high-swept-gain Ni-like Ag XRL in Ref. [15]. As shown in Fig. 4, the simulation results support our considering the low-gain regime as unsaturated or weakly saturated and the high-gain regime as fully saturated.

It should be stressed that the present simulation is not for faithfully reproducing the dominance of one polarization component over the other but for analyzing the effect of phase correlation. The simulation assumes a uniform isotropic medium and one-dimensional propagation. As a consequence, the energy ratio averaged over many runs is nearly 1, although the energy ratio for a single run (corresponding to a single shot in the experiments) can differ significantly from 1 due to the random character of the noise: $\langle I_s \rangle \simeq \langle I_p \rangle$ in Figs. 5 and 6.

The simulation results for the low-gain regime are shown in Fig. 5. The unsaturated status of the simulation results was confirmed from Fig. 4 and explains the substantial relative fluctuation in the total energy [$\delta(I_p + I_s)/\langle I_p + I_s \rangle = 0.23$]. A substantial difference between $\mathcal{P}$ and $\mathcal{P}_u$ ($\langle \mathcal{P} \rangle - \langle \mathcal{P}_u \rangle = 0.36$) is clearly seen in the figure, indicating that a significant level of phase correlation exists ($\langle \rho \rangle = 0.39$). The run number 6 demonstrates an extreme case, where s and p polarization components are almost equal in energy, giving negligible $\mathcal{P}_u$,

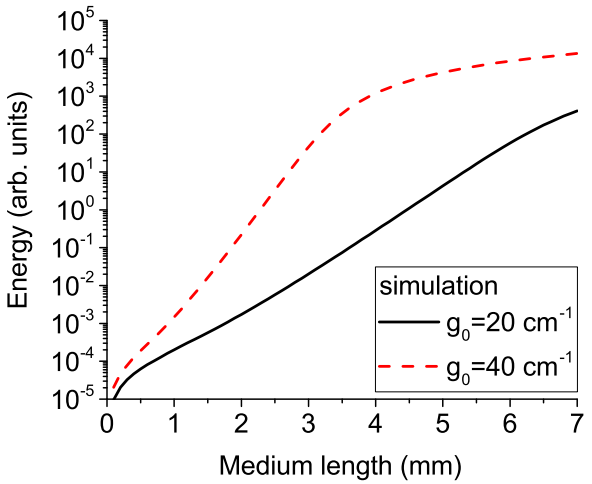

FIG. 4. (Color online) Energy vs medium length for the low-gain regime ($g_0 = 20$ cm^{-1}, black solid line) and the high-gain regime ($g_0 = 40$ cm^{-1}, red dotted line), obtained from the simulations using Maxwell-Bloch equations.

but the true DOP $\mathcal{P}$ is high due to a high degree of phase correlation ($r = 1.01, \mathcal{P}_u = 0.005, \mathcal{P} = 0.76, \rho = 0.57$). This specific polarization state is an elliptical polarization. Another interesting observation is that $\delta\mathcal{P}$ is the same as $\delta\mathcal{P}_u$, although the former is affected not only by δr but also by $\delta\rho$. It suggests that a high degree of phase correlation reduces the fluctuation caused by δr and $\delta\rho$, making DOP more stable. From these observations it is clear that phase correlation is an essential element in analyzing polarization of coherently amplified radiation.

Such a strong phase correlation is induced not by coupling of the transitions responsible for s and p polarization components but by the phase smoothening effect in amplification

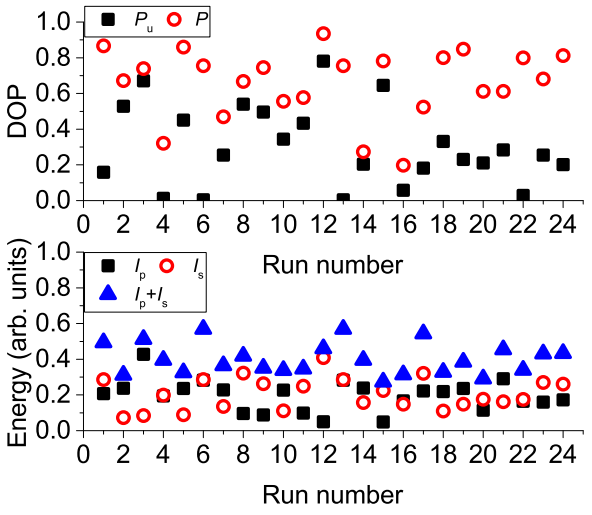

FIG. 5. (Color online) Simulation of XRL polarization for the low-gain regime ($g_0 = 20$ cm^{-1}, $l = 7$ mm): (a) DOP and (b) the energy in each polarization component and the total energy. The descriptive statistics of the data are as follows: $\langle\mathcal{P}\rangle = 0.66$, $\delta\mathcal{P} = 0.19$, $\langle\mathcal{P}_u\rangle = 0.30$, $\delta\mathcal{P}_u = 0.22$, $\langle I_p\rangle = 0.20$, $\delta I_p = 0.09$, $\langle I_s\rangle = 0.21$, $\delta I_s = 0.09$, $\langle I_p + I_s\rangle = 0.40$, and $\delta(I_p + I_s) = 0.09$.

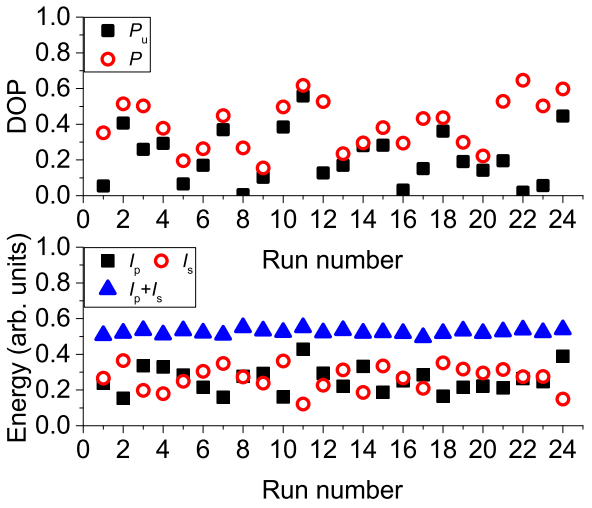

FIG. 6. (Color online) Simulation of XRL polarization for the high-gain regime ($g_0 = 40$ cm^{-1}, $l = 7$ mm): (a) DOP and (b) the energy in each polarization component and the total energy. The descriptive statistics of the data are as follows: $\langle\mathcal{P}\rangle = 0.40$, $\delta\mathcal{P} = 0.14$, $\langle\mathcal{P}_u\rangle = 0.21$, $\delta\mathcal{P}_u = 0.15$, $\langle I_p\rangle = 0.26$, $\delta I_p = 0.07$, $\langle I_s\rangle = 0.27$, $\delta I_s = 0.07$, $\langle I_p + I_s\rangle = 0.52$, and $\delta(I_p + I_s) = 0.01$. The energy scale in this figure is larger than that in Fig. 5 by 25 times.

and temporally localized gain [15]. In the unsaturated regime, the atomic transitions related to the s and p polarization components are virtually independent of each other, and they hardly affect the dynamics of the population inversion. In such a case, the radiation field given at the exit plane can be expressed as a weighted spatiotemporal integration of the radiation field at the prior points and moments. Consequently, although the radiation field originates from noise, once it is amplified, not only does its amplitude grow and smoothen but also its phase smoothens. Furthermore, a gain of a finite duration forces the s polarization signal and p polarization signal to grow in the same temporal range. Any two signals of a smoothly varying phase should have a significant phase correlation when they are overlapping each other temporally. Therefore the growth of phase correlation should be considered as a natural intrinsic feature of wave amplification.

The simulation results for the high-gain regime are shown in Fig. 6. The saturation status of the simulation results was confirmed in the same way as before and explains the high stability of XRL energy [$\delta(I_p + I_s)/\langle I_p + I_s\rangle = 0.02$]. A noticeable difference between $\langle\mathcal{P}\rangle$ and $\langle\mathcal{P}_u\rangle$ [$\langle\mathcal{P}\rangle - \langle\mathcal{P}_u\rangle = 0.19$] still implies a significant degree of phase correlation [$\langle\rho\rangle = 0.12$], and $\delta\mathcal{P}$ still almost equals $\delta\mathcal{P}_u$. However, the phase correlation is smaller than that of the low-gain regime, and consequently, $\langle\mathcal{P}\rangle$, $\langle\mathcal{P}_u\rangle$, $\langle\mathcal{P}\rangle - \langle\mathcal{P}_u\rangle$, and $\langle\rho\rangle$ are smaller than those of the low-gain regime [$\triangle\langle\mathcal{P}\rangle = 0.26$, $\triangle\langle\mathcal{P}_u\rangle = 0.09$, $\triangle(\langle\mathcal{P}\rangle - \langle\mathcal{P}_u\rangle) = 0.17$, and $\triangle\langle\rho\rangle = 0.27$, where $\triangle$ means the difference between the two parameter values estimated for the two regimes]. Since $\langle r\rangle \simeq 1$ in our one-dimensional simulation, the decrease of $\langle\mathcal{P}\rangle$ is mostly due to the decrease of phase correlation.

The reduction of phase correlation in the saturation regime is due to the anticorrelated oscillations of $E_s(t)$ and $E_p(t)$ [15]. In the saturation regime, the strong Rabi oscillation

between the atomic transition forces $|E_s(t)|$ and $|E_p(t)|$ to oscillate in anticorrelation and $\arg[E_s(t)] - \arg[E_p(t)]$ to keep rapidly varying in time. It means that when the number of s-polarized photons increases, that of p-polarized photons decreases, and vice versa. Consequently, $\langle E_s^*(t)E_p(t)\rangle$, which is proportional to ρ, decreases. The reduction of phase correlation in the saturation regime is a natural intrinsic feature of strong coherent radiation-matter interactions. In plasma media, further reduction may be introduced by fast population balancing among the states of the lower lasing level due to elastic electron scattering [14] or by microfluctuation in magnetic field and density [32]. The population balancing was incorporated phenomenologically into our model in terms of population transfer rates, but the effect was not noticeable since the electron collision frequency in our experimental condition was too small for such an effect to be appreciable. The microfluctuation may be relevant for the XRLs of a shorter wavelength in which the wavelength is comparable to the scale length of the fluctuation or the Debye length, probably in a denser plasma gain medium.

IV. CONCLUSION

We presented the measurement results on the polarization state of the amplified spontaneous emission from a collisionally pumped Ni-like Ag XRL operating in the TCE scheme. It was observed that the polarization state of the output radiation depends strongly on the pumping condition. A high degree of fluctuating DOP and the dominance of s polarization were shown for moderate pumping conditions related to the strong prepulse. For strong pumping conditions, p polarization was found to be dominant. To gain a clear physical understanding of the polarization dependence on the pumping conditions, one needs a further, more detailed investigation. The most popular scheme at present, the grazing incidence pumping (GRIP) scheme [33], shows distinguishable differences from the more traditional pump arrangement, which was utilized in the described experiments. In the GRIP scheme, essentially no energy of the main laser pulse is deposited at the critical surface. Measurements of the polarization state in an XRL pumped in the GRIP geometry could shed more light on the role of plasma hydrodynamics and kinetics in polarization buildup.

We also showed, with the simulations based on Maxwell-Bloch equations, that a high degree of phase correlation is developed in XRL media, and it causes DOP to increase significantly. The reasons for phase correlation are the coherent nature of stimulated emission, spatiotemporal smoothening in pulse propagation, and a finite duration of gain. In the saturation regime, the strong radiation-matter interaction makes the phase correlation weaker by inducing anticorrelated oscillations of the two mutually perpendicular polarization components, so the DOP decreases. Thus the coherent interaction, when it is in the nonperturbatively strong regime involving a significant population variation, weakens some of the wave properties of the resulting radiation.

Combination of the experimental findings and the theoretical ones delivers important practical implications. The energy of an XRL depends on saturation differently from other radiation parameters. Before saturation, the energy, the DOP, and the directionality increase as the medium length increases. Upon saturation, the energy keeps increasing even if at a reduced rate, but the other parameters begin to decline. Hence, a compromise is necessary in determining the saturation level to produce strong XRL pulses with a high degree of beneficial parameters like polarization and coherence. A shallow saturation would be the optimum solution. However, even after such an effort, an XRL in the form of a stand-alone oscillator has limitations in its wave features. The pumping conditions inducing anisotropy may only partly improve the situation. For example, the specific polarization state of an XRL changes from shot to shot, regardless of the level of its DOP. The ultimate solution to this problem would be to use a seed signal of good wave properties, e.g., an atomic high harmonic pulse, as has been widely investigated in the last decade [34–36]. It may lead to a source of strong ultrashort coherent polarized EUV or soft x-ray pulses, a dream tool for resolving the microscopic dynamics of materials. To understand and characterize such a tool, more sophisticated methods should be developed, both in theory and experiment, so that both the wave nature and kinetic nature of the problem can be investigated together.

ACKNOWLEDGMENTS

This research was supported by Ministry of Education, Science and Technology of Korea through the Basic Science Research Program (Contract No. R15-2008-006-03001-0); by Gwangju Institute of Science and Technology through the Top Brand Project; and by IBS (Institute for Basic Science) under Contract No. IBS-R012-D1. H.S. acknowledges support from Japan Atomic Energy Agency.

[1] H. Daido, Rep. Prog. Phys. **65**, 1513 (2002).
[2] P. Jaeglé, *Coherent Sources of XUV Radiation: Soft X-Ray Lasers and High-Order Harmonic Generation* (Springer, New York, 2005).
[3] S. Suckewer and P. Jaeglé, Laser Phys. Lett. **6**, 411 (2009).
[4] K. Namikawa, M. Kishimoto, K. Nasu, E. Matsushita, R. Z. Tai, K. Sukegawa, H. Yamatani, H. Hasegawa, M. Nishikino, M. Tanaka, and K. Nagashima, Phys. Rev. Lett. **103**, 197401 (2009).
[5] F. Brizuela, S. Carbajo, A. Sakdinawat, D. Alessi, D. H. Martz, Y. Wang, B. Luther, K. A. Goldberg, I. Mochi, D. T. Attwood, B. L. Fontaine, J. J. Rocca, and C. S. Menoni, Opt. Express **18**, 14467 (2010).
[6] T. Suemoto, K. Terakawa, Y. Ochi, T. Tomita, M. Yamamoto, N. Hasegawa, M. Deki, Y. Minami, and T. Kawachi, Opt. Express **18**, 14114 (2010).
[7] S. Namba, N. Hasegawa, M. Kishimoto, M. Nishikino, K. Takiyama, and T. Kawachi, Phys. Rev. A **84**, 053202 (2011).
[8] H. C. Kang, H. T. Kim, S. S. Kim, C. Kim, T. J. Yu, S. K. Lee, C. M. Kim, I. J. Kim, J. H. Sung, K. A. Janulewicz, J. Lee, and D. Y. Noh, Opt. Lett. **37**, 1688 (2012).

[9] S. Sebban, P. Zeitoun, and A. Klisnick, IEEE Photonics J. **5**, 0700204 (2013).
[10] R. C. Elton, *X-Ray Lasers* (Academic Press, Boston, MA, 1990).
[11] G. J. Tallents, J. Phys. D: Appl. Phys. **36**, R259 (2003).
[12] T. Kawachi, K. Murai, G. Yuan, S. Ninomiya, R. Kodama, H. Daido, Y. Kato, and T. Fujimoto, Phys. Rev. Lett. **75**, 3826 (1995).
[13] B. Rus, C. L. S. Lewis, G. F. Cairns, P. Dhez, P. Jaeglé, M. H. Key, D. Neely, A. G. MacPhee, S. A. Ramsden, C. G. Smith, and A. Sureau, Phys. Rev. A **51**, 2316 (1995).
[14] D. Benredjem, A. Sureau, B. Rus, and C. Möller, Phys. Rev. A **56**, 5152 (1997).
[15] C. M. Kim, K. A. Janulewicz, and J. Lee, Phys. Rev. A **84**, 013834 (2011).
[16] E. Wolf, *Introduction to the Theory of Coherence and Polarization of Light* (Cambridge University Press, Cambridge, MA, 2007).
[17] M. Nishikino, N. Hasegawa, T. Kawachi, H. Yamatani, K. Sukegawa, and K. Nagashima, Appl. Opt. **47**, 1129 (2008).
[18] M. Nishikino, Y. Ochi, N. Hasegawa, T. Kawachi, H. Yamatani, T. Ohba, T. Kaihori, and K. Nagashima, Rev. Sci. Instrum. **80**, 116102 (2009).
[19] F. Delmotte, M.-F. Ravet, F. Bridou, F. Varniere, P. Zeitoun, S. Hubert, L. Vanbostal, and G. Soullie, Appl. Opt. **41**, 5905 (2002).
[20] Y. Ochi, N. Hasegawa, T. Kawachi, and K. Nagashima, Appl. Opt. **46**, 1500 (2007).
[21] Y. Ochi, K. Terakawa, N. Hasegawa, M. Yamamoto, T. Tomita, T. Kawachi, Y. Minami, M. Nishikino, T. Imazono, M. Ishino, and T. Suemoto, Jpn. J. Appl. Phys. **51**, 016601 (2012).
[22] K. A. Janulewicz, C. M. Kim, B. Matouš, H. Stiel, M. Nishikino, N. Hasegawa, and T. Kawachi, in *X-Ray Lasers 2014*, edited by J. Rocca, C. Menoni, and M. Marconi (Springer, Berlin, 2015).
[23] B. L. Henke, E. M. Gullikson, and J. C. Davis, At. Data. Nucl. Data Tables **54**, 181 (1993).
[24] J. Dubau, M. K. Inal, D. Benredjem, and M. Cornille, J. Phys. IV France **11**, Pr2 (2001).
[25] J. C. Kieffer, J. P. Matte, H. Pépin, M. Chaker, Y. Beaudoin, T. W. Johnston, C. Y. Chien, S. Coe, G. Mourou, and J. Dubau, Phys. Rev. Lett. **68**, 480 (1992).
[26] J. C. Kieffer, J. P. Matte, M. Chaker, Y. Beaudoin, C. Y. Chien, S. Coe, G. Mourou, J. Dubau, and M. K. Inal, Phys. Rev. E **48**, 4648 (1993).
[27] A. Ellett, P. D. Foote, and F. L. Mohler, Phys. Rev. **27**, 31 (1926).
[28] H. W. B. Skinner, Roy. Soc. Proc. **A112**, 642 (1926).
[29] J. Dunn, Y. Li, A. L. Osterheld, J. Nilsen, J. R. Hunter, and V. N. Shlyaptsev, Phys. Rev. Lett. **84**, 4834 (2000).
[30] A. Klisnick, J. Kuba, D. Ros, R. Smith, G. Jamelot, C. Chenais-Popovics, R. Keenan, S. J. Topping, C. L. S. Lewis, F. Strati, G. J. Tallents, D. Neely, R. Clarke, J. Collier, A. G. MacPhee, F. Bortolotto, P. V. Nickles, and K. A. Janulewicz, Phys. Rev. A **65**, 033810 (2002).
[31] K. A. Janulewicz, A. Lucianetti, G. Priebe, W. Sandner, and P. V. Nickles, Phys. Rev. A **68**, 051802 (2003).
[32] M. Yu. Romanovsky, J. Ortner, and V. V. Korobkin, J. Phys. IV France **11**, Pr2-293 (2001).
[33] J. Tümmler, K. A. Janulewicz, G. Priebe, and P. V. Nickles, Phys. Rev. E **72**, 037401 (2005).
[34] P. Zeitoun, G. Faivre, S. Sebban, T. Mocek, A. Hallou, M. Fajardo, D. Aubert, P. Balcou, F. Burgy, D. Douillet, S. Kazamias, G. de Lacheze-Murel, T. Lefrou, S. le Pape, P. Mercere, H. Merdji, A. S. Morlens, J. P. Rousseau, and C. Valentin, Nature (London) **431**, 426 (2004).
[35] Y. Wang, E. Granados, F. Pedaci, D. Alessi, B. Luther, M. Berrill, and J. J. Rocca, Nat. Photonics **2**, 94 (2008).
[36] L. M. Meng, D. Alessi, O. Guilbaud, Y. Wang, M. Berrill, B. Luther, S. R. Domingue, D. H. Martz, D. Joyeux, S. D. Rossi, J. J. Rocca, and A. Klisnick, Opt. Express **19**, 12087 (2011).